11-14-2022

Theoretical spectra and energetics for c-C3HC2H, l-C5H2, and bipyramidal D3h C5H2

Alexandria G. Watrous
University of Mississippi

Brent R. Westbrook
University of Mississippi

Ryan C. Fortenberry
University of Mississippi

Recommended Citation

Watrous, A. G., Westbrook, B. R., & Fortenberry, R. C. (2022). Theoretical spectra and energetics for c-C3HC2H, l-C5H2, and bipyramidal D3h C5H2. Frontiers in Astronomy and Space Sciences, 9, 1051535. https://doi.org/10.3389/fspas.2022.1051535

frontiers | Frontiers in Astronomy and Space Sciences

TYPE Original Research
PUBLISHED 14 November 2022
DOI 10.3389/fspas.2022.1051535

OPEN ACCESS

EDITED BY
Mattia Melosso,
Scuola Superiore Meridionale, Italy

REVIEWED BY
Silvia Alessandrini,
Scuola Normale Superiore, Italy
Qian Gou,
Chongqing University, China

*CORRESPONDENCE
Ryan C. Fortenberry,
r410@olemiss.edu

SPECIALTY SECTION
This article was submitted to Astrochemistry,
a section of the journal Frontiers in Astronomy and Space Sciences

RECEIVED 22 September 2022
ACCEPTED 25 October 2022
PUBLISHED 14 November 2022

CITATION
Watrous AG, Westbrook BR and Fortenberry RC (2022), Theoretical spectra and energetics for c-C_3HC_2H, l-C_5H_2, and bipyramidal D_{3h} C_5H_2.
Front. Astron. Space Sci. 9:1051535.
doi: 10.3389/fspas.2022.1051535

Theoretical spectra and energetics for *c*-C_3HC_2H, *l*-C_5H_2, and bipyramidal D_{3h} C_5H_2

Alexandria G. Watrous, Brent R. Westbrook and Ryan C. Fortenberry*

Department of Chemistry and Biochemistry, The University of Mississippi, Oxford, MS, United States

The recent astronomical detection of *c*-C_3HC_2H and *l*-C_5H_2 has led to increased interest in C_5H_2 isomers and their relative stability. The present work provides the first complete list of anharmonic vibrational spectral data with infrared intensities for three such isomers as well as including the first set of rotational data for the bipyramidal C_5H_2 isomer allowing for these molecules to serve as potential tracers of interstellar carbon. All three isomers have fundamental vibrational frequencies with at least one notably intense fundamental frequency. The *l*-C_5H_2 isomer has, by far, the highest intensities out of the three isomers at 2076.3 cm^{-1} (738 km mol^{-1}) and 1887.5 cm^{-1} (182 km mol^{-1}). The *c*-C_3HC_2H isomer has one intense peak at 3460.6 cm^{-1} (84 km mol^{-1}), and the bipyramidal C_5H_2 isomer has one intense peak at 489.3 cm^{-1} (78 km mol^{-1}). The relative intensities highlight that while *l*-C_5H_2 is not the lowest energy isomer, its notable intensities should make it more detectable in the infrared than the lower energy *c*-C_3HC_2H form. The bipyramidal isomer is firmly established here to lie 44.98 kcal mol^{-1} above the cyclic form. The explicitly correlated coupled cluster rovibrational spectral data presented herein should assist with future laboratory studies of these C_5H_2 isomers and aid in detection in astronomical environments especially through the newly operational James Webb Space Telescope.

KEYWORDS

rotational spectroscopy, vibrational spectroscopy, infrared observations, coupled cluster theory, astrochemistry, carbon chemistry

1 Introduction

The unidentified infrared bands (UIRs) are unattributed spectral features observed in virtually all types of astronomical objects whose provenance is not firmly established (Peeters et al., 2002). The UIRs were first recognized in 1973 in the 8–13 μm region and have since been detected in nebulae and in the diffuse interstellar medium (ISM) among other astronomical environments (Peeters et al., 2002). The UIRs were first believed to originate from mostly grain mantle molecules (Allamandola et al., 1979). However, since 1984 most of the UIR spectral features have been hypothesized to be caused

by polycyclic aromatic hydrocarbons (PAHs) (Leger and Puget, 1984; Sellgren, 1984; Molster et al., 2001). One difficulty with supporting this so-called PAH hypothesis is that most PAHs are not rotationally active at worst or weakly dipolar at best. This leads many PAHs to be poor candidates for rotational astronomical detection, which has been the primary vehicle for most astrochemical molecular observation including the recent detection of PAH-like molecules (Cabezas et al., 2021; Cernicharo et al., 2021). However, some small PAH-like molecules, like isomers of C_5H_2, have a lower symmetry which can allow for a nonzero dipole moment and possible rotational activity. Recently, two isomers of C_5H_2, *l*-C_5H_2 and ethynyl cyclopropenylidene (*c*-C_3HC_2H), have been independently detected in Taurus Molecular Cloud-1 and pathways of formation have been determined experimentally and supported theoretically (He et al., 2020; Cabezas et al., 2021; Cernicharo et al., 2021; Karton and Thimmakondu, 2022). The detection of C_5H_2 isomers could allude to other rotationally dark PAHs lurking in the interstellar medium. Insight into the presence, and identity, of PAHs in various astronomical environments can shed light on the chemical and physical aspects of these environments and how they contribute to the UIRs (Tielens, 2008). Additionally the recently launched *James Webb Space Telescope* (JWST) will allow for more detections through vibrational/infrared spectroscopy which can be used for the detection of PAHs that previously could not be detected through rotational spectroscopy.

In addition to the astronomical interest, previous theoretical works have disagreed about the relative energy of C_5H_2 isomers. These have been quantum chemically computed using coupled cluster theory at the CCSD/DZP, CCSD/TZ2P, and CCSD(T)/cc-pVTZ levels, but there are still discrepancies in the relative energies (Balaji and Michl, 1988; Seburg et al., 1997; Veis et al., 2008). Specifically, the bipyramidyl C_5H_2 isomer, shown in **Figure 1**, has an inconsistent magnitude of relative energy when compared to other C_5H_2 isomers depending on the level of theory utilized (Balaji and Michl, 1988; Seburg et al., 1997; Veis et al., 2008). A previous study at the HF/6-31G* level (Pople et al., 1993) places bipyramidal C_5H_2 100 kcal mol^{-1} higher than other C_5H_2 isomers while another study utilizing MBPT(2)/6-31G* puts the bipyramidal C_5H_2 isomer only 30 kcal mol^{-1} higher (Balaji and Michl, 1988; Pople et al., 1993; Seburg et al., 1997). Furthermore, previous density functional and coupled cluster theory computations also place the bipyramidyl C_5H_2 isomer 47–70 kcal mol^{-1} higher than other isomers (Seburg et al., 1997; Karton and Thimmakondu, 2022). Despite the different levels of theory agreeing that the bipyramidyl C_5H_2 isomer is not the lowest energy isomer, there is a clear disagreement on the magnitude of energy difference for the isomer (Balaji and Michl, 1988; Pople et al., 1993; Seburg et al., 1997; Karton and Thimmakondu, 2022). Determining more accurate relative energies is necessary because the ambient energy in the ISM allows for the formation of non-global-minimum structures. However, the energy can not be too much higher; a higher energy difference closer to 100 kcal mol^{-1} is much more unreasonable for formation in the ISM (Seburg et al., 1997). Newer, higher-level computations could help to settle the disagreements as to the relative energy of the bipyramidal C_5H_2 structure compared to the other isomers of C_5H_2. A further look into the *l*-C_5H_2 isomer, shown in **Figure 2**, and the *c*-C_3HC_2H isomer, shown in **Figure 3**, can provide a common reference to determine the relative energy of the bipyramidal C_5H_2 isomer. Additionally the *c*-C_3HC_2H isomer and the *l*-C_5H_2 isomer have been detected in the laboratory by Fourier transform spectrometry which provides a benchmark to the theoretical methods utilized herein (McCarthy et al., 1997; Travers et al., 1997).

The present work utilizes high level quantum chemical computations to compute molecular structures, energies, and spectroscopic data for the bipyramidal C_5H_2 isomer shown in **Figure 1**, the *l*-C_5H_2 isomer shown in **Figure 2**, and the *c*-C_3HC_2H isomer shown in **Figure 3**. The spectroscopic data is computed using quartic force fields (QFFs) which are fourth-order Taylor series expansions of the internuclear potential energy portion of the Watson Hamiltonian (Fortenberry and Lee, 2019). QFFs based on coupled cluster theory at

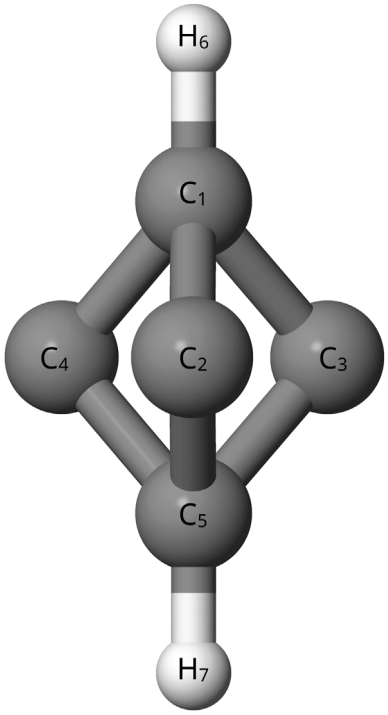

FIGURE 1
Bipyramidal C_5H_2.

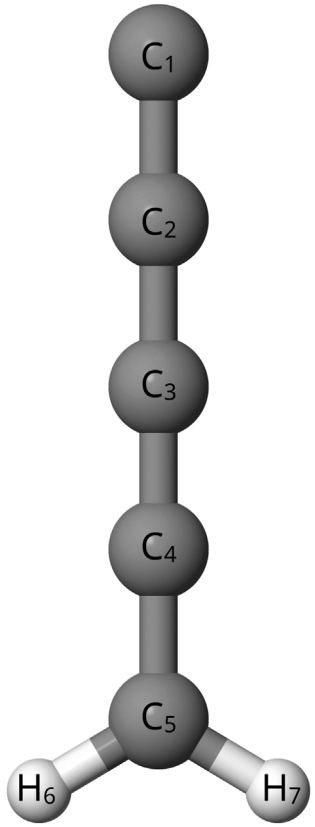

FIGURE 2
l-C_5H_2.

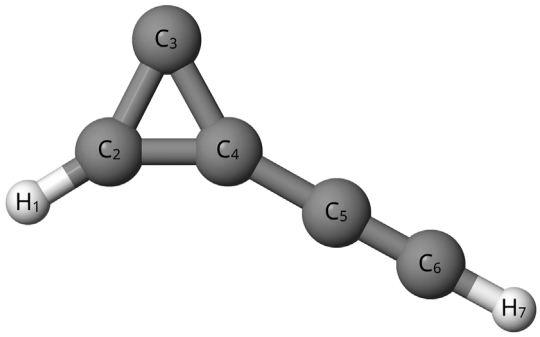

FIGURE 3
c-C_3HC_2H.

the singles, doubles, and perturbative triples level within the explicitly correlated F12b construction [CCSD(T)-F12b] (Adler et al., 2007; Knizia et al., 2009) and a triple-ζ basis set can frequently achieve agreement to within 5–7 cm^{-1} of gas-phase experimental vibrational frequencies (Gardner et al., 2021). However a shortcoming of this method is that the rotational constants are only accurate to about 60 MHz (Agbaglo et al., 2019; Agbaglo and Fortenberry, 2019a,b; Watrous et al., 2021). An improvement would be to utilize a composite method combining core-correlated CCSD(T)-F12b with the cc-pCVTZ-F12 basis set and a correction for scalar relativity (Watrous et al., 2021). This method is referred to as F12-TZ-cCR and offers closer agreement, compared to previous methods, to experimental rotational constants on the order of 7.5 MHz which is necessary for accurate detection (Westbrook et al., 2021b; Watrous et al., 2021). Thus the fundamental vibrational frequencies and rotational constants at this level of theory provided here will lend theoretical support to experiments that will help NASA missions such as the *Stratospheric Observatory for Infrared Astronomy* (SOFIA) and JWST to facilitate the detection of these isomers in space.

2 Computational details

All four levels of theory in the present work utilize CCSD(T)-F12b (Raghavachari et al., 1989; Adler et al., 2007; Knizia et al., 2009; Shavitt and Bartlett, 2009). The first two QFFs use the cc-pV*X*Z-F12 basis sets (Peterson et al., 2008; Yousaf and Peterson, 2008; Knizia et al., 2009) where *X* is D or T. This combination is abbreviated as F12-*X*Z in the following. F12-DZ and F12-TZ QFFs are utilized for all three isomers. The other two levels of theory are based on core-correlated CCSD(T)-F12b with the cc-pCVXZ-F12 basis sets, (Watrous et al., 2021), where *X* is again D or T. Additionally this method includes a correction for scalar relativity computed with canonical CCSD(T) with a cc-pVTZ-DK basis set (Douglas and Kroll, 1974; Jansen and Hess, 1989). This combination is hereafter referred to as F12-*X*Z-cCR. F12-DZ-cCR and F12-TZ-cCR QFFs are only utilized for the *c*-C_3HC_2H isomer due to the substantial increase in computational cost. The QFF for the *c*-C_3HC_2H isomer is composed of 20,641 displacements from the equilibrium geometry along the symmetry-internal coordinates (SICs) shown below with atom labels corresponding to **Figure 3**.

$$S_1(a') = r(H_1 - C_2) \quad (1)$$

$$S_2(a') = r(C_2 - C_3) \quad (2)$$

$$S_3(a') = r(C_3 - C_4) \quad (3)$$

$$S_4(a') = r(C_4 - C_5) \quad (4)$$

$$S_5(a') = r(C_4 - C_6) \quad (5)$$

$$S_6(a') = r(C_4 - H_7) \quad (6)$$

TABLE 1 Relative energy of C_5H_2 Isomers in kcal mol^{-1} compared to previous experiment.

Isomer	F12-DZ	F12-TZ	CCSD(T)/cc-pVTZ[a]	CCSDT(Q)/CBS[b]
c-C_3HC_2H	0.00	0.00	2.01	0.66
l-C_5H_2	13.86	13.79	13.82	13.53
bipyramidyl C_5H_2	45.90	44.98		47.51

[a]From Ref. (Seburg et al., 1997) where energies are relative to a lower energy isomer.
[b]From Ref. (Karton and Thimmakondu, 2022) where energies are relative to a lower energy isomer.

TABLE 2 Rotational constants of *l*-C_5H_2 compared to previous experiment[a].

		F12-DZ		F12-TZ	
Constant	Units	0.005	0.010	0.005	Exp.[a]
A_e	MHz	290162.5	290162.5	290123.6	
B_e	MHz	2290.1	2290.1	2296.4	
C_e	MHz	2272.1	2272.1	2278.4	
A_0	MHz	286248.3	286245.9	287832.8	277600
B_0	MHz	2294.6	2294.5	2307.8	2304.7844
C_0	MHz	2275.7	2275.7	2286.9	2285.8053
D_J	Hz	92.822	92.831	91.191	104
D_{JK}	kHz	70.773	71.920	2,642.5	46.4
D_K	MHz	22.182	22.180	19.676	
d_1	mHz	−771.6	−771.6	−775.9	
d_2	mHz	−285.6	−282.0	1,081.6	
H_J	nHz	−558.98	−516.46	−216,800	
H_{JK}	mHz	238.14	232.78	11,321	
H_{KJ}	kHz	−1.8080	−1.4656	−478.98	
H_K	kHz	6.9698	6.6280	484.19	
h_1	nHz	−50.873	−105.28	−36970	
h_2	mHz	1.1503	1.0644	−0.015785	
h_3	nHz	121.91	115.04	−2042.6	
μ	D			5.94	
κ		−0.99987	−0.99987	−0.99985	

[a]From McCarthy et al., 1997.

$$S_7(a') = \angle(H_1 - C_2 - C_3) \quad (7)$$

$$S_8(a'') = \angle(C_2 - C_3 - C_4) \quad (8)$$

$$S_9(a'') = \angle(C_3 - C_4 - C_5) \quad (9)$$

$$S_{10}(a'') = \angle(C_3 - C_4 - C_6) \quad (10)$$

$$S_{11}(a'') = \angle(C_3 - C_4 - H_7) \quad (11)$$

$$S_{12}(a'') = \tau(H_1 - C_2 - C_3 - C_4) \quad (12)$$

$$S_{13}(a') = \tau(C_2 - C_3 - C_4 - C_5) \quad (13)$$

$$S_{14}(a'') = \tau(C_2 - C_3 - C_4 - C_6) \quad (14)$$

$$S_{15}(a') = \tau(C_2 - C_3 - C_4 - H_7) \quad (15)$$

The QFFs for the *l*-C_5H_2 and bipyramidal C_5H_2 isomers are run directly in Cartesian coordinates composed of 46,064 points and 38,968 points respectively. This increase in the number of points for Cartesians instead of SICs exacerbates the increase in computational cost that would be needed for the F12-DZ-cCR and F12-TZ-cCR methods. For the SIC-based QFFs, the geometry is first optimized at each of the four levels of theory, then each geometry is displaced by 0.005 Å or 0.005 radians along the SICs to form the QFF. For the *c*-C_3HC_2H isomer, in addition to the previous displacements, the out-of-plane bends (OPB) are instead displaced by 0.010 Å or 0.010 radians to help combat the well-known OPB problem (Westbrook et al., 2020; Lee and Fortenberry, 2021). At each of the displaced geometries, single-point energies are calculated. The resulting energies are then fit by a least-squares procedure to yield the optimized geometry. A refit to the function minimum zeroes the gradients and yields the new equilibrium geometry as well as the corresponding force constants. The force constants are then converted from SICs to Cartesian coordinates by using the INTDER program (Allen and coworkers, 2005). For the Cartesian QFFs, each geometry is first optimized at the F12-DZ and F12-TZ levels of theory. Then, each geometry is displaced by 0.005 Å along the Cartesian *x*, *y*, and *z* axes. For *l*-C_5H_2 at the F12-DZ level of theory, each geometry was displaced by 0.010 Å in the out-of-plane coordinates. The force constants are computed numerically by central finite differences (Westbrook et al., 2021b).

For all of the QFFs, the rovibrational spectral data is computed using the SPECTRO software package (Gaw et al., 1991) which uses the Cartesian force constants in vibrational perturbation theory at second order (Watson, 1977; Papousek and Aliev, 1982; Franke et al., 2021) and second-order rotational perturbation theory (Mills, 1972). Type-1 and -2 Fermi resonances, Fermi polyads (Martin and Taylor, 1997) and Coriolis resonances are taken into account to further increase the accuracy of the rovibrational data (Martin et al., 1995; Martin and Taylor, 1997). These are shown in **Supplementary Tables S1–S3** of the Supplemental Information (SI) along with the optimized

TABLE 3 Rotational constants of c-C_3HC_2H compared to previous experiment[a].

		F12-DZ		F12-DZ-cCR		F12-TZ	F12-TZ-cCR	
Constant	**Units**	**0.005**	**0.010**	**0.005**	**0.010**	**0.010**	**0.010**	**Exp.[a]**
A_e	MHz	34593.7	34593.7	34768.1	34768.1	34629.3	34835.3	
B_e	MHz	3410.1	3410.1	3424.5	3424.5	3413.1	3429.6	
C_e	MHz	3104.1	3104.1	3117.5	3,117.5	3106.7	3122.3	
A_0	MHz	34386.9	34398.1	34578.6	34578.7	34449.4	34654.1	34638.701
B_0	MHz	3406.0	3406.2	3420.9	3420.7	3409.9	3426.0	3424.8768
C_0	MHz	3095.8	3096.1	3,109.8	3109.6	3099.6	3114.6	3113.6386
D_J	Hz	245.00	245.00	246.72	246.71	244.68	246.14	288
D_K	kHz	29.813	29.801	29.780	29.788	29.659	29.795	29.5
D_{JK}	kHz	105.97	105.80	107.72	106.72	105.79	106.57	
d_1	Hz	−28.524	−28.523	−28.662	−28.663	−28.472	−28.589	
d_2	Hz	−19.625	−19.617	−19.581	−19.586	−19.524	−19.570	
H_J	μHz	−173.88	−173.55	−172.98	−172.73	−170.73	−171.01	
H_{JK}	mHz	106.73	106.531	106.24	105.97	104.63	105.22	
H_{KJ}	Hz	−4.0028	−3.9978	−3.9473	−3.9491	−3.8877	−39.167	
H_K	Hz	4.0870	4.0827	4.0363	4.0384	3.9812	40.157	
h_1	μHz	−13.184	−13.165	−13.022	−13.040	−12.987	−12.952	
h_2	μHz	90.284	90.145	89.750	89.589	88.667	88.905	
h_3	μHz	18.237	18.222	18.092	18.098	17.999	18.007	
μ	D					3.59		
κ		−0.98018	−0.98019	−0.98023	−0.98023	−0.9802	−0.98025	

[a]From Travers et al., 1997.

TABLE 4 Rotational constants of bipyramidal C_5H_2.

Constant	**Units**	**F12-DZ**	**F12-TZ**
B_e	MHz	12733.1	12742.1
C_e	MHz	9145.2	9153.0
B_0	MHz	12647.4	12656.6
C_0	MHz	9055.4	9063.7
D_J	KHz	2.979	2.979
D_{JK}	kHz	6.770	6.718
D_K	kHz	1.676	1.751
d_1	mHz	48.6	2.06
d_2	mHz	8.42	1.21
H_J	mHz	1.736	1.746
H_{JK}	mHz	−10.886	−11.033
H_{KJ}	mHz	9.011	9.935
H_K	mHz	21.254	20.669
h_1	μHz	0.702	−1.215
h_2	μHz	1.282	−2.913
h_3	μHz	263.914	257.523

geometrical parameters and T_1 diagnostics shown in **Supplementary Tables S4–S6**. The anharmonic zero point vibrational energy (ZPVE) from the refit geometry, refit energy (only for the SIC QFF), and energy from the optimized minima are added together to calculate the relative energy.

The geometry optimizations, harmonic frequencies, single point energies, and dipole moments are computed using the Molpro 2020.1 software package (Werner et al., 2020). The dipole moments are computed at the F12-TZ level of theory. Double-harmonic and anharmonic infrared intensities are computed using Gaussian16 (Frisch et al., 2016) with the MP2/aug-cc-pVTZ (Møller and Plesset, 1934; Kendall et al., 1992), B3LYP/aug-cc-pVTZ (Yang et al., 1986; Lee et al., 1988; Becke, 1993), and B3LYP/N07D (Barone et al., 2008) levels of theory. Previous work has shown semi-quantitative accuracy for harmonic infrared intensities for the MP2 level of theory for a substantial decrease in cost relative to higher-level computations (Yu et al., 2015; Finney et al., 2016; Westbrook et al., 2021a).

3 Results and discussion

The relative energies of l-C_5H_2, c-C_3HC_2H, and bipyramidal C_5H_2 are compared at the F12-DZ and the F12-TZ levels of theory as shown in **Table 1**. The relative energies of the c-C_3HC_2H and l-C_5H_2 isomers are similar to previous (Seburg et al., 1997) relative energy computations with the l-C_5H_2 isomer being 13.79 kcal mol^{-1} higher in energy than the c-C_3HC_2H isomer. However, the bipyramidal C_5H_2 isomer is lower in relative energy

TABLE 5 F12-DZ and F12-TZ harmonic and fundamental vibrational frequencies and B3LYP/N07D intensities (in km mol^{-1}) of l-C_5H_2 compared to previous theory computed at the fc-CCSD(T)/cc-pVTZ level of theory[b].

		F12-DZ		F12-TZ	B3LYP/N07D		Previous theory[b]	
	Description	0.005	0.010	0.005	Freq	f	Freq	f
$\omega_1(b_2)$	C-H Anti-Sym Stretch	3,219.4	3219.4	3215.5	3,199.1	1	3,215.1	0.0
$\omega_2(a_1)$	C-H Sym Stretch	3127.7	3127.7	3125.1	3117.5	1	3127.3	0.6
$\omega_3(a_1)$	(C_1-C_2) - (C_2-C_3) + (C_3-C_4) - (C_4-C_5)	2145.3	2,145.3	2,153.5	2212.7	806	2,151.6	677.1
$\omega_4(a_1)$	(C_1-C_2) - (C_2-C_3) - (C_3-C_4) + (C_4-C_5)	1924.4	1924.4	1935.2	1974.6	206	1921.8	176.6
$\omega_5(a_1)$	H-C-C Sym Bend	1503.9	1503.9	1506.9	1513.8	9	1,503.5	7.7
$\omega_6(a_1)$	(C_1-C_2) + (C_2-C_3) - (C_3-C_4) - (C_4-C_5)	1349.5	1349.5	1355.8	1369.9	7	1346.9	18.0
$\omega_7(b_2)$	H-C-C Anti-Sym Bend	1033.7	1,033.7	1030.7	1031.0	1	1030.3	0.4
$\omega_8(b_1)$	C_5 OPB	936.0	936.3	941.4	968.6	34	943.4	31.6
$\omega_9(a_1)$	(C_1-C_2) + (C_2-C_3) + (C_3-C_4) + (C_4-C_5)	749.0	749.0	752.2	769.8	1	745.5	0.4
$\omega_{10}(b_1)$	C_3-C_4 OPB	534.0	534.3	536.1	656.4	7	576.2	2.8
$\omega_{11}(b_2)$	C_2-C_3 IPB	398.4	398.4	411.7	527.6	4	445.4	0.9
$\omega_{12}(b_1)$	C_2-C_4 OPB	244.8	244.7	239.9	314.8	7	270.9	8.5
$\omega_{13}(b_2)$	C_2-C_4 IPB	231.1	231.1	230.9	286.2	7	254.9	5.7
$\omega_{14}(b_2)$	C_1-C_5 IPB	133.3	133.3	123.2	148.3	1	139.3	0.0
$\omega_{15}(b_1)$	C_1 OPB	110.8	110.7	104.3	143.7	2	122.3	3.1
ZPVE		8758.4	8812.5	8948.0				
$\nu_1(b_2)$	C-H Anti-Sym Stretch	3073.7	3066.1	3078.2	3047.4	1		
$\nu_2(a_1)$	C-H Sym Stretch	3019.2	3011.6	2,955.4	3013.1	2		
$\nu_3(a_1)$	(C_1-C_2) - (C_2-C_3) + (C_3-C_4) - (C_4-C_5)	2098.9	2090.6	2076.3	2170.4	738		
$\nu_4(a_1)$	(C_1-C_2) - (C_2-C_3) - (C_3-C_4) + (C_4-C_5)	1898.0	1894.9	1887.5	1944.1	182		
$\nu_5(a_1)$	H-C-C Sym Bend	1472.0	1467.4	1,43.8	1483.5	6		
$\nu_6(a_1)$	(C_1-C_2) + (C_2-C_3) - (C_3-C_4) - (C_4-C_5)	1340.7	1334.1	1318.9	1350.5	6		
$\nu_7(b_2)$	H-C-C Anti-Sym Bend	1022.5	1018.7	1155.4	1011.6	1		
$\nu_8(b_1)$	C_5 OPB	924.6	923.8	769.0	944.8	35		
$\nu_9(a_1)$	(C_1-C_2) + (C_2-C_3) + (C_3-C_4) + (C_4-C_5)	741.0	730.1	756.4	772.4	1		
$\nu_{10}(b_1)$	C_3-C_4 OPB	534.0[a]	534.3[a]	536.1[a]	365.8	7		
$\nu_{11}(b_2)$	C_2-C_3 IPB	398.4[a]	398.4[a]	411.7[a]	285.8	2		
$\nu_{12}(b_1)$	C_2-C_4 OPB	224.8[a]	244.7[a]	239.9[a]	244.3	4		
$\nu_{13}(b_2)$	C_2-C_4 IPB	231.1[a]	231.1[a]	230.9[a]	247.5	9		
$\nu_{14}(b_2)$	C_1-C_5 IPB	133.3[a]	133.3[a]	123.2[a]	151.6	1		
$\nu_{15}(b_1)$	C_1 OPB	110.8[a]	110.7[a]	104.3[a]	133.7	2		

[a]Harmonic values reported.
[b]Previous theory from Karton and Thimmakondu, 2022.

than some previous computations (Balaji and Michl, 1988; Pople et al., 1993; Seburg et al., 1997). The relative energy of the bipyramidal C_5H_2 isomer at the F12-TZ level of theory is 44.98 kcal mol^{-1} compared to the c-C_3HC_2H isomer. This relative energy is much closer to the previous MBPT(2)/6-31G* calculations, at about 30 kcal mol^{-1}, as opposed to previous calculations at the HF/6-31G* level of theory where the relative energy was roughly 100 kcal mol^{-1} higher than other C_5H_2 isomers (Balaji and Michl, 1988; Pople et al., 1993; Seburg et al., 1997). While this highly-symmetric isomer gives indication of possessing multi-reference effects due to its large T_1 diagnostic (0.059), the extent to which this will affect the relative energies is left for future work.

3.1 Rotational constants

Out of the three isomers, the l-C_5H_2 isomer has the largest dipole moment of 5.94 D and its equilibrium ($_e$) and vibrationally-averaged ($_0$) rotational constants, shown in **Table 2**, demonstrate near prolate character (κ = − 0.99987 for the F12-TZ level of theory, where κ is defined as $(2B_0 - A_0 - C_0)/(A_0 - C_0)$). This large dipole moment has helped with detection of the molecule through rotational spectroscopy. The F12-DZ and F12-TZ rotational constants agree well with a maximum relative difference of 0.57% in the B_0 rotational constant. Compared to experimental Fourier transform microwave spectroscopy (McCarthy et al., 1997), the F12-TZ B_0 and C_0 rotational constants differ from experiment by only 3.0 MHz (0.13%) and 1.1 MHz (0.05%) respectively. This benchmarking constrains the expected accuracy for other, unknown spectral observables provided in this work. The A_0 rotational constant differs from experiment by 10,200 MHz (3.67%), but the error for the A_0 rotational constant is known to have a higher error for near prolate molecules (Gardner et al., 2021). The complete set of the vibrationally excited rotational constants are reported in **Supplementary Table S7** of the SI. The quartic and sextic distortion constants in the S-reduced Hamiltonian are reported

TABLE 6 Harmonic and fundamental vibrational frequencies of c-C_3HC_2H compared to previous theory computed at the fc-CCSD(T)/cc-pVTZ level of theory[b].

		F12-DZ		F12-DZ-cCR		F12-TZ	F12-TZ-cCR	Previous Theory[b]
	Description	0.005	0.010	0.005	0.010	0.010	0.010	
$\omega_1(a')$	Acetylene C-H Stretch	3454.7	3454.7	3459.8	3459.8	3,454.2	3460.6	3457.0
$\omega_2(a')$	Ring CH Stretch	3261.1	3261.1	3266.4	3266.4	3,259.9	3266.7	3261.4
$\omega_3(a')$	C_5 In-Plane Motion	2166.4	2166.4	2172.6	2172.6	2,167.9	2176.2	2163.8
$\omega_4(a')$	C_4-C_5 Out-of-Plane Motion	1713.4	1713.4	1719.3	1719.3	1715.1	1722.9	1708.0
$\omega_5(a')$	(C_2-C_3) + (C_3-C_4) Stretch	1278.5	1,278.6	1,283.9	1283.9	1279.7	1286.5	1269.8
$\omega_6(a')$	(C_2-C_3) - (C_3-C_4) Stretch	1117.4	1117.4	1122.5	1122.5	1119.8	1126.1	1107.9
$\omega_7(a')$	C_3-C_2-H_1 IPB	949.9	949.9	953.8	953.8	948.5	952.3	945.8
$\omega_8(a'')$	C_3-C_2-H_1 OPB	892.9	893.2	895.9	895.9	893.7	898.2	891.2
$\omega_9(a'')$	C_5-C_6-H_7 OPB	710.0	710.0	714.8	714.8	713.9	717.8	705.4
$\omega_{10}(a')$	C_4-C_5 Stretch	696.0	696.0	698.6	698.6	697.5	700.9	692.1
$\omega_{11}(a')$	C_5-C_6-H_7 IPB	604.4	604.4	608.7	608.7	611.3	615.6	601.8
$\omega_{12}(a'')$	C_4-C_5 Out-Of Plane Motion	510.4	510.4	511.6	511.6	517.7	521.7	520.4
$\omega_{13}(a')$	C_4-C_5 In Plane Motion	498.8	498.8	502.4	502.4	504.3	508.9	500.1
$\omega_{14}(a'')$	C_5-C_6 Out-Of-Plane Motion	201.8	201.8	202.8	202.7	202.6	203.6	212.9
$\omega_{15}(a')$	C_5-C_6 In-Plane Motion	189.2	189.2	190.7	190.7	190.8	192.0	193.0
ZPVE		7869.7	8908.0	9383.5	9115.5	9234.5	9069.4	
$\nu_1(a')$	Acetylene C-H Stretch	3412.6	3341.7	3311.3	3328.8	3346.4	3347.8	
$\nu_2(a')$	Ring CH Stretch	3034.4	3,102.4	3137.1	3139.1	3145.4	3,127.1	
$\nu_3(a')$	C_5 In-Plane Motion	2168.0	2131.8	2,123.4	2,128.7	2,124.3	2135.5	
$\nu_4(a')$	C_4-C_5 Out-of-Plane Motion	1673.6	1675.5	1675.2	1681.4	1685.3	1706.8	
$\nu_5(a')$	(C_2-C_3) + (C_3-C_4) Stretch	1138.0	1,199.5	1,262.1	1,265.1	1,285.6	1256.3	
$\nu_6(a')$	(C_2-C_3) - (C_3-C_4) Stretch	1194.6	1,113.6	1073.5	1090.0	1073.9	1061.0	
$\nu_7(a')$	C_3-C_2-H_1 IPB	949.9[a]	891.7	944.2	958.9	948.5[a]	916.2	
$\nu_8(a'')$	C_3-C_2-H_1 OPB	892.9[a]	848.5	895.9[a]	865.1	893.7[a]	898.2[a]	
$\nu_9(a'')$	C_5-C_6-H_7 OPB	710.0[a]	684.7	711.6	689.8	705.2	646.6	
$\nu_{10}(a')$	C_4-C_5 Stretch	696.0[a]	698.2	675.1	690.3	674.7	700.9[a]	
$\nu_{11}(a')$	C_5-C_6-H_7 IPB	555.1	574.6	574.4	585.6	595.0	577.9	
$\nu_{12}(a'')$	C_4-C_5 Out-Of Plane Motion	510.4[a]	510.4[a]	511.6[a]	511.6[a]	517.7[a]	521.7[a]	
$\nu_{13}(a')$	C_4-C_5 In Plane Motion	498.8[a]	476.6	502.1	506.6	504.3[a]	500.7	
$\nu_{14}(a'')$	C_5-C_6 Out-Of-Plane Motion	201.8[a]	201.8[a]	202.8[a]	202.7[a]	202.6[a]	203.6[a]	
$\nu_{15}(a')$	C_5-C_6 In-Plane Motion	189.2[a]	189.2[a]	190.7[a]	190.7[a]	190.8[a]	169.5	

[a]Harmonic values reported.
[b]Previous theory from Karton and Thimmakondu, 2022.

in **Table 2**. The D_J constant is about 13 Hz lower than experiment while the D_{JK} constant differs from experiment by around 24 kHz at the F12-DZ level of theory, but has a much higher difference at the F12-TZ level of theory at around 2,596 kHz. While D_{JK} often exhibits minor effects on the rotational spectrum of near-prolate molecules (Stein et al., 2015), this erroneous l-C_5H_2 D_{JK} value for F12-TZ (and, in fact, all of its sextic distortion constants, as well) presently stems from a compounding error brought about by the step size and the resulting QFF improperly representing these data. The F12-DZ data are consistent within step size and experimental comparison implying that these data are reliable as are the F12-TZ data behaving in similar ways.

The c-C_3HC_2H isomer has a smaller dipole moment than the l-C_5H_2 isomer at 3.59 D. The c-C_3HC_2H isomer also shows near prolate character (κ = − 0.98026 at the F12-TZ-cCR level of theory) as exhibited by the rotational constants B_0 and C_0 being almost the same as shown in **Table 3**. The F12-TZ-cCR data agrees extremely well with previous Fourier transform spectrometry results (Travers et al., 1997), differing by only 1.1 MHz (0.03%) for the B_0 rotational constant, 0.96 MHz (0.03%) for the C_0 rotational constant, and even 15 MHz (0.04%) for the A_0 rotational constant. Both the F12-DZ-cCR and F12-TZ-cCR methods produce rotational constants closer to experiment than F12-DZ and F12-TZ which in line with previous work (Watrous et al., 2021). Doubling the step size for the OBPs has little-to-no effect in the rotational constants as expected. The S-reduced Hamiltonian quartic and sextic distortion constants are reported in **Table 3**, and the D_K constant compares well with experiment, only differing by 0.2 kHz at the F12-TZ-cCR level of theory. The experimental D_J rotational constant is 288 Hz while the computed D_J rotational constant is 246.14 Hz. However, the computed A-reduced Hamiltonian Δ_J, determined in this work, has a value of 285.28 Hz which aligns closely with the reported experimental value, suggesting a potential misattribution in the experimental work.

TABLE 7 Intensities in km mol^{-1} of c-C_3HC_2H compared to previous theory computed at the fc-CCSD(T)/cc-pVTZ level of theory[a].

		MP2/TZ		B3LYP/TZ		B3LYP/N07D		Previous theory[a]
	Description	**Freq**	f	**Freq**	f	**Freq**	f	f
$\omega_1(a')$	Acetylene C-H Stretch	3474.6	85	3461.2	90	3478.7	100	71.1
$\omega_2(a')$	Ring CH Stretch	3283.4	2	3234.4	1	3250.2	1	1.1
$\omega_3(a')$	C_5 In-Plane Motion	2145.1	6	2192.6	3	2193.7	3	10.6
$\omega_4(a')$	C_4-C_5 Out-of-Plane Motion	1703.2	4	1719.7	5	1724.9	6	5.0
$\omega_5(a')$	(C_2-C_3) + (C_3-C_4) Stretch	1286.9	32	1280.3	38	1275.1	39	41.2
$\omega_6(a')$	(C_2-C_3) - (C_3-C_4) Stretch	1128.9	3	1,108.7	8	1103.3	7	6.5
$\omega_7(a')$	C_3-C_2-H_1 IPB	944.6	3	951.9	2	943.8	3	2.3
$\omega_8(a'')$	C_3-C_2-H_1 OPB	902.0	13	899.9	15	880.8	17	17.1
$\omega_9(a'')$	C_5-C_6-H_7 OPB	687.5	31	756.5	27	744.4	36	28.7
$\omega_{10}(a')$	C_4-C_5 Stretch	704.2	2	708.8	1	706.5	1	1.7
$\omega_{11}(a')$	C_5-C_6-H_7 IPB	614.5	45	610.1	54	595.4	65	49.2
$\omega_{12}(a'')$	C_4-C_5 Out-Of Plane Motion	531.9	2	549.5	5	562.2	2	1.9
$\omega_{13}(a')$	C_4-C_5 In Plane Motion	503.0	3	530.7	4	538.2	2	2.4
$\omega_{14}(a'')$	C_5-C_6 Out-Of-Plane Motion	206.5	1	218.6	1	238.4	1	0.9
$\omega_{15}(a')$	C_5-C_6 In-Plane Motion	188.0	7	202.3	7	211.9	6	5.7
$\nu_1(a')$	Acetylene C-H Stretch	3,351.6	78	3,335.6	81	3353.6	84	
$\nu_2(a')$	Ring CH Stretch	3,156.9	1	3106.0	1	3117.9	1	
$\nu_3(a')$	C_5 In-Plane Motion	2113.8	3	2152.0	2	2152.1	2	
$\nu_4(a')$	C_4-C_5 Out-of-Plane Motion	1667.0	3	1,677.7	4	1681.0	4	
$\nu_5(a')$	(C_2-C_3) + (C_3-C_4) Stretch	1253.1	29	1,249.3	36	1245.1	34	
$\nu_6(a')$	(C_2-C_3) - (C_3-C_4) Stretch	1107.2	1	1078.6	3	1075.4	3	
$\nu_7(a')$	C_3-C_2-H_1 IPB	921.5	4	930.7	3	922.3	4	
$\nu_8(a'')$	C_3-C_2-H_1 OPB	886.1	13	885.1	15	871.0	20	
$\nu_9(a'')$	C_5-C_6-H_7 OPB	673.0	31	742.5	28	691.3	30	
$\nu_{10}(a')$	C_4-C_5 Stretch	703.3	1	696.9	1	696.1	1	
$\nu_{11}(a')$	C_5-C_6-H_7 IPB	613.0	43	592.7	55	555.0	52	
$\nu_{12}(a'')$	C_4-C_5 Out-Of Plane Motion	532.8	3	545.0	4	508.1	1	
$\nu_{13}(a')$	C_4-C_5 In Plane Motion	497.4	4	526.4	4	491.7	9	
$\nu_{14}(a'')$	C_5-C_6 Out-Of-Plane Motion	210.5	1	220.2	1	212.0	1	
$\nu_{15}(a')$	C_5-C_6 In-Plane Motion	192.2	7	201.7	7	195.7	5	

[a]Previous theory from Karton and Thimmakondu, 2022.

Unlike the other two isomers, the bipyramidal C_5H_2 isomer does not have a dipole due to its D_{3h} symmetry. Even so, the rotational constants for the bipyramidal C_5H_2 isomer are given in **Table 4** for completeness. Additionally, the molecule is oblate and has only B_0 and C_0 rotational constants. The bipyramidal C_5H_2 molecule has not been detected in astrophysical observations or even observed experimentally. The F12-DZ and the F12-TZ methods have good agreement differing by only 9.2 MHz for the C_0 rotational constant. Hence, the results presented here provide the most accurate predictions of its rotational constants which may be helpful for the accurate kinetic rate determination or the thermochemical analysis that requires the full rotational partition function.

3.2 Vibrational frequencies

The l-C_5H_2 isomer has the largest anharmonic intensities out of the three C_5H_2 isomers, as shown in **Table 5**. The two most intense modes are ν_3 with an intensity of 738 km mol^{-1} at 2076.3 cm^{-1} (4.81 μm) and ν_4 with an intensity of 182 km mol^{-1} at 1887.5 cm^{-1} (5.30 μm). These intensities represent the movements in the linear carbon chain and are up to ten times larger than the anti-symmetric stretch in water, which has an intensity of about 70 km mol^{-1} at the same level of theory. The large intensities of these two frequencies imply that l-C_5H_2 should be observable right at the edge of the NIRspec instrument onboard JWST in a region often bereft of known transitions for organic molecules. Out of the three levels of theory in this work used to compute intensities, only the B3LYP/N07D results are reported for the l-C_5H_2 isomer as it is the only method with all real frequencies in line with the present high-level computations. The previous theory used to compute the intensities agrees qualitatively with the order of intensities computed with B3LYP/N07D. Additionally, the N07D basis set is designed to handle hydrocarbon systems like this and has been used to produce anharmonic frequencies in reasonable agreement with experiment (Barone et al., 2008; Barone et al., 2013). However in this case, the anharmonic frequencies produced by B3LYP/N07D fall short in comparison with the fundamental frequencies produced by the F12-TZ level of theory. In contrast, the F12-DZ and F12-TZ anharmonic frequencies have relatively close agreement. The exceptions to this are the modes involving an in-plane bend (IPB) or OPB of

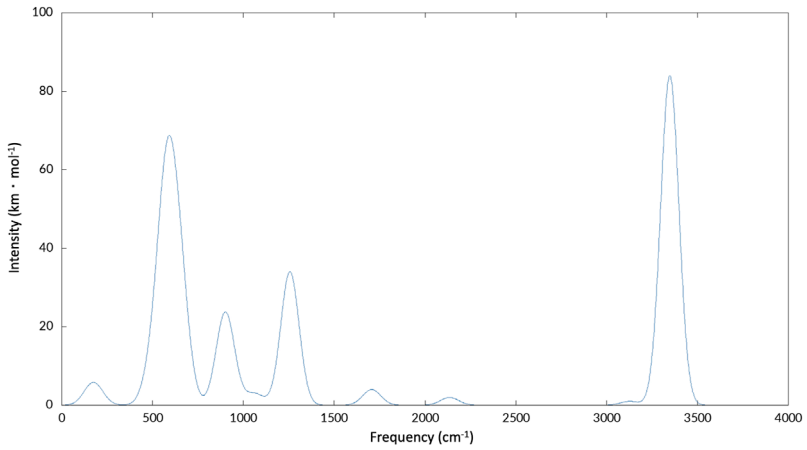

FIGURE 4
Simulated spectrum of *c*-C_3HC_2H.

TABLE 8 F12-DZ and F12-TZ harmonic and fundamental frequencies of bipyramidal C_5H_2 with intensities in km mol^{-1} compared to previous theory computed at the fc-CCSD(T)/cc-pVTZ level of theory[a].

		F12-DZ	F12-TZ	MP2/TZ		B3LYP/TZ		B3LYP/N07D		Previous theory[a]	
	Description			**Freq**	***f***	**Freq**	***f***	**Freq**	***f***	**Freq**	***f***
ω_1 (a_1')	C-H Sym Stretch	3331.6	3329.5	3376.0	–	3311.0	–	3319.9	–	3331.6	0.0
ω_2 (a_2'')	C-H Anti-Sym Stretch	3330.0	3327.8	3,374.7	30	3309.4	11	3318.5	9	3330.0	12.3
ω_3 (a_1')	C_1-C_5 Stretch	1307.1	1308.7	1,302.2	–	1314.5	–	1329.5	–	1299.7	0.0
ω_4 (a_2'')	C_1-C Ring - C_5-C Ring Stretch	1288.3	1290.4	1,298.0	29	1,289.5	28	1302.8	24	1276.2	19.6
$\omega_5(e')$	H-CC Sym Bend	1128.2	1126.8	1079.6	5	1129.2	10	1136.8	10	1129.0	8.3
$\omega_6(e'')$	H-CC Anti-Sym Bend	1010.9	1008.3	978.1	–	1017.8	–	1,024.1	–	1011.5	0.0
ω_7 (a_1')	C_1-C_2,C_3,C_4-C_5 Stretch	852.2	851.5	913.1	–	837.5	–	834.4	–	846.8	0.0
$\omega_8(e')$	C_2-C_3 - C_2-C_4 Stretch	842.5	844.1	813.4	30	850.4	15	857.5	16	839.4	20.4
$\omega_9(e'')$	C_1-C_2 - C_2-C_5 Stretch	783.8	786.2	807.0	–	734.2	–	771.1	–	777.1	0.0
$\omega_{10}(e')$	C_2-C_3 + C_2-C_4 Stretch	488.7	489.3	382.4	82	525.9	48	530.7	46	490.7	49.9
ZPVE		9228.0	9187.4								
ν_1 (a_1')	C-H Sym Stretch	3190.5	3190.4	3,240.7	1	3187.4	1	3189.1	1		
ν_2 (a_2'')	C-H Anti-Sym Stretch	3146.4	3139.3	3239.6	30	3187.0	10	3188.8	7		
ν_3 (a_1')	C_1-C_5 Stretch	1250.9	1253.0	1271.2	1	1262.9	1	1283.3	1		
ν_4 (a_2'')	C_1-C Ring - C_5-C Ring Stretch	1273.4	1273.6	1269.6	27	1318.5	27	1334.3	23		
$\nu_5(e')$	H-CC Sym Bend	1126.4	1108.7	1048.7	5	1103.8	9	1108.7	11		
$\nu_6(e'')$	H-CC Anti-Sym Bend	1009.1	995.2	953.7	–	1001.5	–	1001.2	-		
ν_7 (a_1')	C_1-C_2,C_3,C_4-C_5 Stretch	834.4	832.4	914.3	1	850.4	3	847.0	1		
$\nu_8(e')$	C_2-C_3 - C_2-C_4 Stretch	830.1	829.5	800.2	30	836.9	12	842.3	14		
$\nu_9(e'')$	C_1-C_2 - C_2-C_5	756.3	759.2	770.8	–	719.7	–	752.9	–		
$\nu_{10}(e')$	C_2-C_3 + C_2-C_4	452.6	426.1	344.9	78	524.2	50	526.6	47		

[a]Previous theory from Karton and Thimmakondu, 2022.

the carbon chain, ν_{10}-ν_{15}. The portions of the QFF involving these modes have problems with the cubic and quartic force constants. Those modes are reported as the harmonic values, and most anharmonic corrections are within the margin of error for the levels of theory. A larger step size is also used at the F12-DZ level of theory to combat the OPB problem (Fortenberry et al., 2018; Westbrook et al., 2020; Lee and Fortenberry, 2021; Lee and Fortenberry, 2021). However there is no significant improvement of the issue. As a result, the larger step size is not repeated for the F12-TZ level of theory. This will not affect possible detection *via* JWST because the NIRSpec and MIRI instruments on the JWST only capture spectra to about 333 cm^{-1}, but the resolution drops for the lower frequencies below 2000 cm^{-1} since the larger range MIRI instrument does not have the same capabilities as NIRspec. The harmonic frequencies for both the F12-DZ and F12-TZ levels of theory agree well with previous theoretical harmonic

frequencies for most modes (Karton and Thimmakondu, 2022), but vary more for the OPB and IPB which is likely due to the aforementioned OPB problem (Westbrook et al., 2020; Lee and Fortenberry, 2021).

For the *c*-C_3HC_2H isomer, the vibrational frequencies are in **Table 6**, and the double-harmonic intensities are in **Table 7**. The *c*-C_3HC_2H isomer has two intense peaks with the most intense peak being the acetylene C-H stretch, ν_1, at 3,347.8 cm^{-1} (2.99 μm) with an anharmonic intensity of 84 km mol^{-1} at the B3LYP/N07D level of theory. The second most intense peak is the C_5-C_6-H_7 in-plane bend (IPB), ν_{11}, at 577.9 cm^{-1} (17.3 μm) with an intensity of 52 km mol^{-1}. The intensity changes depending on which level of theory is used to calculate the double-harmonic intensities, but all three methods computed for the intensities agree on the qualitative order of intensities for the modes, as does the previous theory (Karton and Thimmakondu, 2022). The intensities for *c*-C_3HC_2H are not as strong as the intensities for *l*-C_5H_2, but are still strong enough for detection.

For the *c*-C_3HC_2H, there are differences in the anharmonic frequencies between the levels of theory and step sizes as shown in **Table 6**. Fundamental frequencies ν_{12}, ν_{14}, and ν_{15} produce questionable positive anharmonicities, although they are below or on the lower edge of the range to be detected through the aforementioned instruments on JWST. Additionally, these three modes have a maximum intensity of 5 km mol^{-1}. Both considerations make these frequencies unlikely to be detected. Increasing the level of theory to F12-DZ-cCR improves the anharmonic correction for the ν_9, ν_{10}, and ν_{13} fundamentals. The doubled step size in the OPB coordinates further improves the anharmonic correction for F12-DZ and F12-DZ-cCR. As a result only the doubled step size is calculated at the higher levels of theory due to the increased computational cost. Similarly, this doubled step size helps the anharmonic correction for ν_7 and ν_8 with F12-DZ and F12-DZ-cCR. There is much less variation in the harmonic frequencies between the levels of theory. Additionally, the harmonic frequencies compare well to previous theory (Karton and Thimmakondu, 2022). **Figure 4** shows a simulated spectrum of the F12-TZ-cCR anharmonic frequencies and the B3LYP/N07D intensities with all bands incorporated; only those with notable intensities are present.

For the bipyramidal C_5H_2 isomer, the vibrational frequencies for the F12-DZ and F12-TZ QFFs, shown in **Table 8**, have close agreement for most of the frequencies. The bipyramidal C_5H_2 isomer has one intense frequency in which is ν_{10}, the symmetric C_2-C_3 + C_2-C_4 stretch, with an intensity of 78 km mol^{-1} at 426.1 cm^{-1} (23.5 μm) which is slightly smaller than the *c*-C_3H_2H isomer and much smaller than the most intense peaks for the *l*-C_5H_2 isomer. Unlike the other isomers, the bipyramidal C_5H_2 isomer only has three other fundamentals that have intensities over 10 km mol^{-1} at the B3LYP/N07D level of theory. These are ν_4 at 1,273.6 cm^{-1} (7.85 μm), ν_5 at 1,108.7 cm^{-1} (9.02 μm), and ν_8 at 829.5 cm^{-1} (12.0 μm). While the different methods differ in the quantitative value of the intensities, they again agree qualitatively with each other and with previous theory on what will be the most and least intense peaks (Karton and Thimmakondu, 2022). However only having one fundamental with a large intensity could increase the difficulty for the detection of the bipyramidal C_5H_2 isomer compared to the other two isomers. The F12-DZ and the F12-TZ QFFs show good agreement for the harmonic and anharmonic fundamental frequencies and the harmonic frequencies further show good agreement to previous theory (Karton and Thimmakondu, 2022). The largest discrepancy arises in ν_{10}, with a difference of 26.5 cm^{-1}, but a majority of the frequencies agree to within 3 cm^{-1}. However, given the greater computational rigor of F12-TZ, its data should be considered the more reliable of the two.

4 Conclusion

The large intensities for some of the fundamental frequencies in all of the isomers may facilitate the detection of these C_5H_2 structures *via* JWST. Such spectral data could lead to the identification for some UIRs as well as unknown transitions of known interstellar molecules such as *l*-C_5H_2 and *c*-C_3HC_2H. The bipyramidal C_5H_2 isomer has some of the lowest intensities of the three isomers but still has one peak at 426.1 cm^{-1} (23.5 μm) with an intensity of 78 km mol^{-1}. The *c*-C_3HC_2H isomer has one intense fundamental frequency at 3,347.8 cm^{-1} with an intensity of 84 km mol^{-1}. The *l*-C_5H_2 isomer has the two highest intensities out of the three isomers for its ν_4 at 1887.5 cm^{-1} with a large intensity of 182 km mol^{-1} and ν_3 at 2076.3 cm^{-1} with a very large intensity of 738 km mol^{-1} making this fundamental the most likely of the group especially since, again, *l*-C_5H_2 has been previously detected *via* radioastronomy. The F12-TZ methodology produces rotational constants for *l*-C_5H_2 within 3 MHz (0.13%) for the B_0 and C_0 rotational constants. Improving upon this high level of accuracy, the F12-TZ-cCR methodology for *c*-C_3HC_2H produces B_0 and C_0 rotational constants within 1.1 MHz (0.03%) of experiment. This close agreement to experiment lends supports to the accuracy of the other theoretical values, notably the fundamental vibrational frequencies, reported herein. Out of the three C_5H_2 isomers presented in this work, the *c*-C_3HC_2H isomer has the lowest relative energy, with *l*-C_5H_2 13.79 kcal mol^{-1} higher in line with previous work (Seburg et al., 1997). The bipyramidal C_5H_2 isomer is 44.98 kcal mol^{-1} higher in energy compared previous computations which places this D_{3h} isomer 100 kcal mol^{-1} or more higher than other C_5H_2 isomers (Seburg et al., 1997). The dipole moments for the *c*-C_3HC_2H and *l*-C_5H_2 isomers are large at 3.59 D and 5.94 D, respectively, which has facilitated the previous detections of the isomers in space through rotational spectroscopy. Overall, the anharmonic vibrational frequencies and rotational constants presented herein may help

to facilitate the laboratory or astronomical detection of unknown transitions of known molecules. In particular, the high-intensity fundamental frequencies of each molecule that fall within the high-resolution range of JWST may also help to disentangle some of the heretofore unidentified features in the UIRs.

Data availability statement

The original contributions presented in the study are included in the article/**Supplementary Material**, further inquiries can be directed to the corresponding author.

Author contributions

AW, BW, and RF contributed to conception and design of the study. AW performed the computations. AW and BW analyzed the data. AW wrote the first draft of the manuscript, and BW and RF edited the manuscript. RF secured funding for the research and provided administration for the project. All authors contributed to manuscript revision, read, and approved the submitted version.

Acknowledgments

The authors wish to acknowledge funding from NASA grant NNX17AH15G, NSF grant CHE-1757888, NSF grant OIA-1757220, and the University of Mississippi's College of Liberal Arts as well as computational resources from the Mississippi Center for Supercomputing Research (MCSR).

Conflict of interest

The authors declare that the research was conducted in the absence of any commercial or financial relationships that could be construed as a potential conflict of interest.

Publisher's note

All claims expressed in this article are solely those of the authors and do not necessarily represent those of their affiliated organizations, or those of the publisher, the editors and the reviewers. Any product that may be evaluated in this article, or claim that may be made by its manufacturer, is not guaranteed or endorsed by the publisher.

Supplementary Material

The Supplementary Material for this article can be found online at: https://www.frontiersin.org/articles/10.3389/fspas.2022.1051535/full#supplementary-material

References

Adler, T. B., Knizia, G., and Werner, H.-J. (2007). A simple and efficient CCSD(T)-F12 approximation. *J. Chem. Phys.* 127, 221106. doi:10.1063/1.2817618

Agbaglo, D., and Fortenberry, R. C. (2019b). The performance of explicitly correlated wavefunctions [CCSD(T)-F12b] in the computation of anharmonic vibrational frequencies. *Chem. Phys. Lett.* 734, 136720. doi:10.1016/j.cplett.2019.136720

Agbaglo, D., and Fortenberry, R. C. (2019a). The performance of explicitly correlated methods for the computation of anharmonic vibrational frequencies. *Int. J. Quantum Chem.* 119, e25899. doi:10.1002/qua.25899

Agbaglo, D., Lee, T. J., Thackston, R., and Fortenberry, R. C. (2019). A small molecule with PAH vibrational properties and a detectable rotational spectrum: *c*-(C)C_3H_2, cyclopropenylidenyl carbene. *Astrophys. J.* 871, 236. doi:10.3847/1538-4357/aaf85a

Allamandola, L. J., Greenberg, J. M., and Norman, C. A. (1979). On the middle infra-red fluorescence and absorption of molecules in grain mantles. *Astron. Astrophys.* 77, 66–74.

Allen, W. D., and coworkers (2005). *INTDER 2005 is a general program written by W. D. Allen and coworkers, which performs vibrational analysis and higher-order non-linear transformations*, Athens, GA: University of Georgia.

Balaji, V., and Michl, J. (1988). New strained organic molecules: Theory guides experiment. *Pure Appl. Chem.* 60, 189–194. doi:10.1351/pac198860020189

Barone, V., Biczysko, M., Bloino, J., Egidi, F., and Puzzarini, C. (2013). Accurate structure, thermodynamics, and spectroscopy of medium-sized radicals by hybrid coupled cluster/density functional theory approaches: The case of phenyl radical. *J. Chem. Phys.* 138 (23), 234303.

Barone, V., Cimino, P., and Stendardo, E. (2008). Development and validation of the B3LYP/N07D computational model for structural parameter and magnetic tensors of large free radicals. *J. Chem. Theory Comput.* 4, 751–764. doi:10.1021/ct800034c

Becke, A. D. (1993). Density-functional thermochemistry. III. the role of exact exchange. *J. Chem. Phys.* 98, 5648–5652. doi:10.1063/1.464913

Cabezas, C., Tercero, B., Agúndez, M., Marcelino, N., Pardo, J. R., de Vicente, P., et al. (2021). Cumulene carbenes in TMC-1: Astronomical discovery of *l*-H_2C_5. *Astron. Astrophys.* 650, L9. doi:10.1051/0004-6361/202141274

Cernicharo, J., Agúndez, M., Cabezas, C., Tercero, B., Marcelino, N., Pardo, J. R., et al. (2021). Pure hydrocarbon cycles in TMC-1: Discovery of ethynyl cyclopropenylidene, cyclopentadiene, and indene. *Astron. Astrophys.* 649, L15. doi:10.1051/0004-6361/202141156

Douglas, M., and Kroll, N. (1974). Quantum electrodynamical corrections to the fine structure of helium. *Ann. Phys. (N. Y).* 82, 89–155. doi:10.1016/0003-4916(74)90333-9

Finney, B., Fortenberry, R. C., Francisco, J. S., and Peterson, K. A. (2016). A spectroscopic case for SPSi detection: The third-row in a single molecule. *J. Chem. Phys.* 145, 124311. doi:10.1063/1.4963337

Fortenberry, R. C., and Lee, T. J. (2019). Computational vibrational spectroscopy for the detection of molecules in space. *Ann. Rep. Comput. Chem.* 15, 173–202. doi:10.1016/bs.arcc.2019.08.006

Fortenberry, R. C., Novak, C. M., and Lee, T. J. (2018). Rovibrational analysis of *c*-SiC_2H_2: Further evidence for out-of-plane bending issues in correlated methods. *J. Chem. Phys.* 149, 024303. doi:10.1063/1.5043166

Franke, P. R., Stanton, J. F., and Douberly, G. E. (2021). How to VPT2: Accurate and intuitive simulations of CH stretching infrared spectra using VPT2+K with large effective Hamiltonian resonance treatments. *J. Phys. Chem. A* 125, 1301–1324. doi:10.1021/acs.jpca.0c09526

Frisch, M. J., Trucks, G. W., Schlegel, H. B., Scuseria, G. E., Robb, M. A., Cheeseman, J. R., et al. (2016). *Gaussian 16 revision C.01*. Wallingford CT: Gaussian Inc.

Gardner, M. B., Westbrook, B. R., Fortenberry, R. C., and Lee, T. J. (2021). Highly-accurate quartic force fields for the prediction of anharmonic rotational constants and fundamental vibrational frequencies. *Spectrochimica Acta Part A Mol. Biomol. Spectrosc.* 248, 119184. doi:10.1016/j.saa.2020.119184

Gaw, J. F., Willets, A., Green, W. H., and Handy, N. C. (1991). SPECTRO: A program for the derivation of spectrscopic constants from provided quartic force fields and cubic dipole fields. *Advances in Molecular Vibrations and Collision Dynamics*. Editor Bowman Joel M., and Ratner Mark A. (Greenwich, Connecticut: JAI Press, Inc.), 170–185.

He, C., Galimova, G. R., Luo, Y., Kaiser, R. I., Eckhardt, A. K., Sun, R., et al. (2020). A chemical dynamics study on the gas-phase formation of triplet and singlet C_5H_2 carbenes. *Proc. Natl. Acad. Sci. U. S. A.* 117, 30142–30150. doi:10.1073/pnas.2019257117

Jansen, G., and Hess, B. A. (1989). Revision of the douglas-kroll transformation. *Phys. Rev. A* 39, 6016–6017. doi:10.1103/physreva.39.6016

Karton, A., and Thimmakondu, V. S. (2022). From molecules with a planar tetracoordinate carbon to an astronomically known C_5H_2 carbene. *J. Phys. Chem. A* 126, 2561–2568. doi:10.1021/acs.jpca.2c01261

Kendall, R. A., Dunning, T. H., and Harrison, R. J. (1992). Electron affinities of the first-row atoms revisited. systematic basis sets and wave functions. *J. Chem. Phys.* 96, 6796–6806. doi:10.1063/1.462569

Knizia, G., Adler, T. B., and Werner, H.-J. (2009). Simplified CCSD(T)-F12 methods: Theory and benchmarks. *J. Chem. Phys.* 130, 054104. doi:10.1063/1.3054300

Lee, C., Yang, W. T., and Parr, R. G. (1988). Development of the Colle-Salvetti correlation-energy formula into a functional of the electron density. *Phys. Rev. B* 37, 785–789. doi:10.1103/physrevb.37.785

Lee, T. J., and Fortenberry, R. C. (2021). The unsolved issue with out-of-plane bending frequencies for C C multiply bonded systems. *Spectrochimica Acta Part A Mol. Biomol. Spectrosc.* 248, 119148. doi:10.1016/j.saa.2020.119148

Leger, A., and Puget, J. L. (1984). Identification of the "unidentified IR emission features" of interstellar dust? *Astron. Astrophys.* 137, L5–L8.

Martin, J. M. L., Lee, T. J., Taylor, P. R., and François, J.-P. (1995). The anharmonic force field of ethylene, C_2H_4, by means of accurate *ab initio* calculations. *J. Chem. Phys.* 103, 2589–2602. doi:10.1063/1.469681

Martin, J. M. L., and Taylor, P. R. (1997). Accurate *ab initio* quartic force field for *trans*-HNNH and treatment of resonance polyads. *Spectrochimica Acta Part A Mol. Biomol. Spectrosc.* 53, 1039–1050. doi:10.1016/s1386-1425(96)01869-0

McCarthy, M. C., Travers, M. J., Kovács, A., Gottlieb, C. A., and Thaddeus, P. (1997). Eight new carbon chain molecules. *Astrophys. J. Suppl. Ser.* 113, 105–120. doi:10.1086/313050

Mills, I. M. (1972). "Vibration-rotation structure in asymmetric- and symmetric-top molecules," in *Molecular spectroscopy - modern research*. Editors K. N. Rao, and C. W. Mathews (New York: Academic Press), 115–140.

Møller, C., and Plesset, M. S. (1934). Note on an approximation treatment for many-electron systems. *Phys. Rev.* 46, 618–622. doi:10.1103/physrev.46.618

Molster, F. J., Lim, T. L., Sylvester, R. J., Waters, L. B. F. M., Barlow, M. J., Beintema, D. A., et al. (2001). The complete ISO spectrum of NGC 6302. *Astron. Astrophys.* 372, 165–172. doi:10.1051/0004-6361:20010465

Papousek, D., and Aliev, M. R. (1982). *Molecular vibration-rotation spectra*. Amsterdam: Elsevier.

Peeters, E., Hony, S., Van Kerckhoven, C., Tielens, A. G. G. M., Allamandola, L. J., Hudgins, D. M., et al. (2002). The rich 6 to 9 μm spectrum of interstellar PAHs. *Astron. Astrophys.* 390, 1089–1113. doi:10.1051/0004-6361:20020773

Peterson, K. A., Adler, T. B., and Werner, H.-J. (2008). Systematically convergent basis sets for explicitly correlated wavefunctions: The atoms H, He, B-Ne, and Al-Ar. *J. Chem. Phys.* 128, 084102. doi:10.1063/1.2831537

Pople, J. A., Scott, A. P., Wong, M. W., and Radom, L. (1993). Scaling factors for obtaining fundamental vibrational frequencies and zero-point energies from HF/6-31G* and MP2/6-31G* harmonic frequencies. *Isr. J. Chem.* 33, 345–350. doi:10.1002/ijch.199300041

Raghavachari, K., Trucks, G. W., Pople, J. A., and Head-Gordon, M. (1989). A fifth-order perturbation comparison of electron correlation theories. *Chem. Phys. Lett.* 157, 479–483. doi:10.1016/s0009-2614(89)87395-6

Seburg, R. A., McMahon, R. J., Stanton, J. F., and Gauss, J. (1997). Structures and stabilities of C_5H_2 isomers: Quantum chemical studies. *J. Am. Chem. Soc.* 119, 10838–10845. doi:10.1021/ja971412j

Sellgren, K. (1984). The near-infrared continuum emission of visual reflection nebulae. *Astrophys. J.* 277, 623–633. doi:10.1086/161733

Shavitt, I., and Bartlett, R. J. (2009). *Many-body methods in Chemistry and physics: MBPT and coupled-cluster theory*. Cambridge: Cambridge University Press.

Stein, C., Weser, O., Schroder, B., and Botschwina, P. (2015). High-level theoretical spectroscopic parameters for three ions of astrochemical interest. *Mol. Phys.* 113, 2169–2178. doi:10.1080/00268976.2015.1017019

Tielens, A. G. G. M. (2008). Interstellar polycyclic aromatic hydrocarbon molecules. *Annu. Rev. Astron. Astrophys.* 46, 289–337. doi:10.1146/annurev.astro.46.060407.145211

Travers, M. J., McCarthy, M. C., Gottlieb, C. A., and Thaddeus, P. (1997). Laboratory detection of the ring-chain molecule C_5H_2. *Astrophys. J.* 483, L135–L138. doi:10.1086/310744

Veis, L., Čàrsky, P., Pittner, J., and Michl, J. (2008). Coupled cluster study of polycyclopentanes: Structure and properties of C_5H_{2n}, n = 0-4. *Collect. Czechoslov. Chem. Commun.* 73, 1525–1551. doi:10.1135/cccc20081525

Watrous, A. G., Westbrook, B. R., and Fortenberry, R. C. (2021). F12-TZ-cCR: A methodology for faster and still highly-accurate quartic force fields. *J. Phys. Chem. A* 125, 10532–10540. doi:10.1021/acs.jpca.1c08355

Watson, J. K. G. (1977). "Aspects of quartic and sextic centrifugal effects on rotational energy levels," in *Vibrational spectra and structure*. Editor J. R. During (Amsterdam: Elsevier), 1–89.

Werner, H.-J., Knowles, P. J., Manby, F. R., Black, J. A., Doll, K., Heßelmann, A., et al. (2020). Molpro, version 2020.1, a package of *ab initio* programs. *WIREs Comput. Mol. Sci.* 2, 242–253. See http://www.molpro.net. doi:10.1002/wcms.82

Westbrook, B. R., Del Rio, W. A., Lee, T. J., and Fortenberry, R. C. (2020). Overcoming the out-of-plane bending issue in an aromatic hydrocarbon: The anharmonic vibrational frequencies of c-$(CH)C_3H_2^+$. *Phys. Chem. Chem. Phys.* 22, 12951–12958. doi:10.1039/d0cp01889a

Westbrook, B. R., Patel, D. J., Dallas, J. D., Swartzfager, G. C., Lee, T. J., and Fortenberry, R. C. (2021a). Fundamental vibrational frequencies and spectroscopic constants of substituted cyclopropenylidene (*c*-C_3HX, x=F, Cl, CN). *J. Phys. Chem. A* 125, 8860–8868. doi:10.1021/acs.jpca.1c06576

Westbrook, B. R., Valencia, E. M., Rushing, S. C., Tschumper, G. S., and Fortenberry, R. C. (2021b). Anharmonic vibrational frequencies of ammonia borane (BH_3NH_3). *J. Chem. Phys.* 154, 041104. doi:10.1063/5.0040050

Yang, W. T., Parr, R. G., and Lee, C. T. (1986). Various functionals for the kinetic energy density of an atom or molecule. *Phys. Rev. A* 34, 4586–4590. doi:10.1103/physreva.34.4586

Yousaf, K. E., and Peterson, K. A. (2008). Optimized auxiliary basis sets for explicitly correlated methods. *J. Chem. Phys.* 129, 184108. doi:10.1063/1.3009271

Yu, Q., Bowman, J. M., Fortenberry, R. C., Mancini, J. S., Lee, T. J., Crawford, T. D., et al. (2015). The structure, anharmonic vibrational frequencies, and intensities of $NNHNN^+$. *J. Phys. Chem. A* 119, 11623–11631. doi:10.1021/acs.jpca.5b09682